

Novel method for ecosystem services assessment and analysis of road-effect zones

Hong Zhang^{a,*}, Xin Xu^b, Chi Zhang^{c,d,*}, Zhi-Peng Fu^e, Hong-Zhi Yang^c

^a Transportation Institute, Inner Mongolia University, Hohhot 010020, China

^b Pioneer College, Inner Mongolia University, Hohhot 010020, China

^c Key Laboratory for Special Area Highway Engineering of Ministry of Education, Chang'an University, Xi'an 710064, Shaanxi, China

^d Engineering Research Center of Highway Infrastructure Digitalization, Ministry of Education, Xi'an 710000, Shaanxi, China

^e CCCC First Highway Consultants Co. Ltd., Xi'an 710075, Shaanxi, China

ARTICLE INFO

Keywords:

Green infrastructure
Ecosystem services
Road-effect zone
Soil and water conservation
Habitat quality
Ecologically fragile areas

ABSTRACT

To explore the cumulative ecological effects of roads in ecologically fragile areas, the Integrated Valuation of Ecosystem Services and Trade-offs (InVEST) tool was applied to assess the spatio-temporal changes in habitat quality, water yield, and soil erosion in road-effect zones of the Western Sichuan Plateau, China. Then, generalized estimating equations were formulated to analyze the impact of synergies among road attributes, climate, topography, land cover, and other factors on ecosystem service changes. The results showed that the habitat quality within the road-effect zones was mostly affected by road grade and structure, and water yield and soil erosion were attributed to the factors of road structure, rainfall, and topography. Roadbed sections had the greatest negative impact on ecosystem services, followed by bridge sections and tunnel sections. Overall, the results of this study address habitat encroachment and soil and water loss in ecologically fragile areas, contributing to knowledge on green infrastructure planning.

1. Introduction

Worldwide, urban expansion and economic development have led to a vast number of transport infrastructure projects that are being built or in use. Highways, railways, and other linear infrastructures, however, have introduced environmental problems related to changes in land and topography, such as soil desertification (Cao et al., 2021; Wang et al., 2022), water and land resource shortages (Uliasz-Misiak et al., 2022), biodiversity decline (González-Bernardo et al., 2023; Kroeger et al., 2022; Mulero-Pazmany et al., 2023), and serious degradation of ecosystem services (Arunyawat and Shrestha, 2018; Lisiak-Zielinska et al., 2022). In particular, belt-shaped infrastructure, such as highways, can extend over long distances and traverse diverse geomorphic and ecological regions. The different road structures within the corridor belt, including roadbeds, bridges, and tunnels, present different impacts on the soil, vegetation, waterbodies, topography, and wildlife of the ecosystem.

Specifically, roadbed sections alter the original land cover types, which directly or indirectly leads to habitat loss, landscape connectivity degradation, and reduced biodiversity (Llagostera et al., 2022; Mayer et al., 2022; Rao et al., 2018). The rough soil texture

* Corresponding authors. At: No.49, Xilinguole South Road, Yuquan District, Hohhot 010020, Inner Mongolia, China (H. Zhang). Middle Section of the South Second Ring Road, Yanta District, Xi'an 710064, Shaanxi, China (C. Zhang).

E-mail addresses: hongzhang@chd.edu.cn (H. Zhang), xuxin@chd.edu.cn (X. Xu), zhangchi@chd.edu.cn (C. Zhang), fuzhipeng@ccccltd.cn (Z.-P. Fu), yhz@chd.edu.cn (H.-Z. Yang).

<https://doi.org/10.1016/j.trd.2024.104057>

Received 27 June 2023; Received in revised form 2 December 2023; Accepted 2 January 2024
1361-9209/© 2024 Elsevier Ltd. All rights reserved.

and increased particle sizes such as gravel of the roadbed sections can easily lead to the decline of soil structure and water conservation ability, nutrient loss, followed by the difficulty of vegetation restoration, forming a vicious circle (Hacisalihoglu et al., 2019). In addition, when the excavated road sections are below the groundwater level, water seepage can occur on the slope toe and surface, resulting in reduced underground water and surface vegetation, soil and water loss, or worse, geological disasters such as landslides. In the roadbed sections, fill can raise the upstream groundwater level, lower the downstream level, and destroy the downstream ecological balance. For bridge sections, bridge piers can modify river flow patterns and result in riverbank erosion, increased downstream silt, and flooding (Liang et al., 2018). Some road projects may also alter existing watercourses, with potential long-term negative impacts. For tunnel sections, damage to vegetation and topography is primarily concentrated at the tunnel entrance. Additionally, tunnel excavation may lead to gradual changes in the hydrological cycle, the physical and chemical properties of the soil, and the rate of soil erosion (Lv et al., 2020). Overall, in the entire life cycle of the road, its negative impacts on the ecosystem are mainly manifested as reducing habitat quality and water yield and increasing soil erosion. In China, this situation is more prominent in ecologically fragile areas such as the Qinghai-Tibet Plateau (QTP) due to its high altitude, low heat, strong winds, drought, hypoxia, strong radiation and other natural characteristics (Li et al., 2018). For instance, the Western Sichuan Plateau located on the southeastern edge of the QTP boasts breathtaking natural landscapes, and the flourishing tourism industry has led to the planning and construction of roads and other infrastructure in the area. However, the delicate ecology of the region is threatened by the conflict between road development and ecological conservation.

Planners, builders, and scholars involved in the development of linear transportation infrastructure are increasingly concerned about the relationship between roads and the ecological environment, particularly in ecologically sensitive areas. Recent research in transportation has predominantly focused on the macroscopic perspective, examining the impact of linear infrastructure on landscape patterns such as fragmentation, connectivity, diversity, and habitat loss (Oliveira Gonçalves et al., 2022; Wei et al., 2022; Yan et al., 2023). Additionally, studies have explored the microscopic perspective, investigating topics such as vehicle emissions, green transportation, and the concept of sponge cities (Han et al., 2023; Zhao et al., 2021; Zheng et al., 2022). While these studies have elucidated the environmental impacts of roads, limited research has been conducted on the quantitative assessment and analysis of ecosystem services in dense road network areas. Additionally, the consideration of road factors (such as road grade, structure, length and operation duration) in existing studies tends to be relatively homogeneous.

On the other hand, in the field of road ecology, the geographical areas on both sides of the road centerline that may affect the ecosystem are called road-effect zones (van der Ree et al., 2011). Numerous approaches have been applied to determine the road-effect zone and assess its ecological risk, including field investigation, qualitative assessment, raster statistics, map algebra, multiple regression, and pressure-state-response (Ahhammad et al., 2019; Phillips et al., 2020; Wang et al., 2018; Wu et al., 2021). In China, the approach usually involves qualitatively evaluating the ecological effects of roads according to the Specifications for Environmental Impact Assessment of Highways. The specifications focus on the road impacts to wildlife, borrow pits, slag fields, and land occupation and propose necessary ecological protection and restoration measures by predicting ecosystem resilience. Some scholars have evaluated ecological risks in road-effect zones from the perspective of landscape processes and ecosystem services based on geographic information system (GIS) tools. Zhang et al. (2010) analyzed the impact of road grade and density on landscape patterns using metrics such as landscape fragmentation, aggregation, dominance, vulnerability, and soil erosion. Wu et al. (2014) explored the impact of highways on habitat quality using the Integrated Valuation of Ecosystem Services and Trade-offs (InVEST) approach. The results showed that the habitat quality on the two sides of the road was highly asymmetric due to varied spatial landscape patterns and that preserving farmland and woodland can improve habitat quality and recover rare animals. ZhuGe et al. (2014) evaluated the potential habitat of Tibetan antelope based on the habitat suitability module of the InVEST model, revealing that human disturbance, such as roads and settlements, can lead to serious habitat degradation. Wang et al. (2022) analyzed soil erosion on unpaved roads in the lateritic region of southern China based on the Water Erosion Prediction Project. The above qualitative assessment method focuses on local typical ecological problems and cannot visually display the ecological risks within the road-effect zone. GIS-based models and the InVEST approach can intuitively show the landscape ecological risk and ecosystem service of grids, but they may overlook the impact due to road attribute changes such as grade, structure, length, and operation duration. Moreover, there is a limited number of mathematical modeling studies that quantitatively analyze the synergic ecological effect of roads together with other natural factors.

While previous work mostly evaluated landscape and ecosystem services at the regional level, this study takes a step further to quantitatively assess the impact of road construction on ecosystem services from a meso perspective, accounting for the coupled impact of road attributes (such as road grade, structure, length, and operation duration) and the surrounding natural environment. That is, a quantitative evaluation approach is applied to examine the impact of road-effect zones and road attributes on ecosystem services. Given the limitations of previous qualitative analysis and GIS-based map algebra, this study adopts an innovative approach using InVEST and generalized estimating equations (GEEs). InVEST incorporates several modules covering habitat quality, hydrological services, soil conservation, and so on, which is suitable for addressing the issue of observational data shortages (Arunyawat and Shrestha, 2016; Gurung et al., 2018; Yue et al., 2022). GEEs are statistical models used to analyze repeated-measures data, and they can solve the problem of nonindependence of data and produce robust estimates of parameters (Abbasi & Keshavarzi, 2019; Onder, 2016; Zhang et al., 2020). In terms of contribution, previous studies have proposed certain evaluation methods to reveal the impact of human activities on ecology and landscapes, whereas this paper modifies these methods to make them applicable to the assessment of ecosystem services in road-effect zones. Combining road ecology analysis, the impact mechanism and weight of road and natural attributes on ecosystem services are derived. Furthermore, by analyzing data from multiple roads, it is possible to identify patterns and trends in the provision of ecosystem services. Last, it is envisioned that ecosystem service assessment and analysis within this research context will foster proactive design of road infrastructure and promote ecologically green and sustainable construction technology. By quantifying the impacts of road construction on ecosystem services, decision-makers can make more informed choices and develop

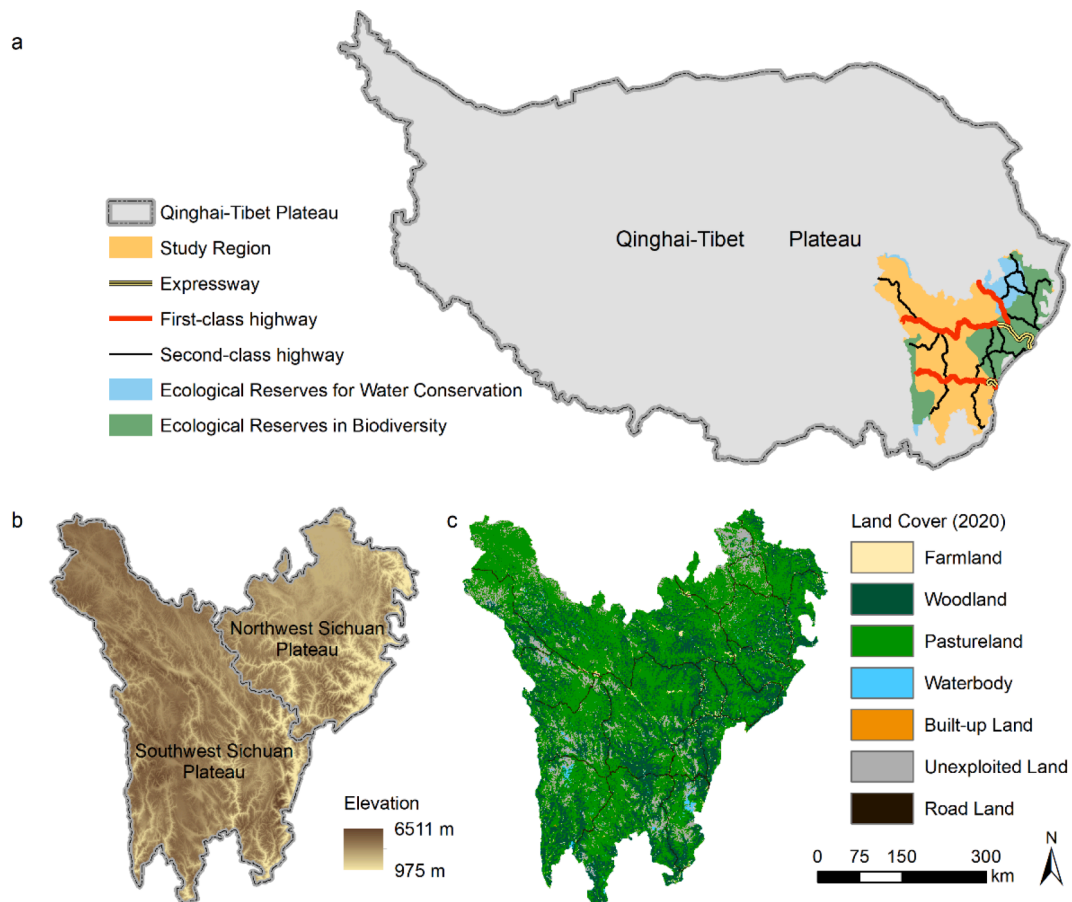


Fig. 1. Geographical location (a), elevation (b) and land cover (c) of the study area.

strategies that minimize negative impacts and maximize the benefits of road development while ensuring the sustainable management of natural resources. This research will provide valuable information for land use planning, conservation strategies, and policy-making processes. It will enhance our understanding of the trade-offs and synergies between road development and the provision of ecosystem services.

The paper is structured as follows. This study selected the Western Sichuan Plateau as the study region. Then, the InVEST models were modified to assess the regional spatiotemporal changes in ecosystem services (i.e., habitat quality, water yield, and soil erosion) from 2010 to 2020. GIS tools were used to extract the assessment results within the road-effect zone. Finally, certain GEEs were formulated to analyze the synergistic impacts among road attributes, climate, location, topography, soil, land use and other factors on ecosystem service changes.

2. Research methodology

2.1. Study region

The Western Sichuan Plateau, located on the southeastern edge of the QTP (97°–104.5°E, 34°–28°N), is abundant in diverse species, waterways, forests, and other natural resources. The region has established numerous ecological reserves for water and biodiversity conservation (Fig. 1a). However, field investigations have revealed significant ecological challenges stemming from anthropogenic activities such as large-scale hydropower development, agriculture and animal husbandry, infrastructure construction, and urban expansion. These activities have led to habitat degradation, biodiversity decline, conflicts between pastoral development and woodland and biodiversity conservation, reduction in marshes, decreased capacity of woodlands to retain water, severe soil erosion, and degradation of the water environment. Additionally, the region has a higher number of low-grade highways with limited accessibility. Consequently, since 2010, the linear transportation infrastructure in the area has continued to expand, primarily at the expense of grasslands, woodlands, and croplands, exacerbating ecological risks. In summary, the Western Sichuan Plateau was chosen as the study region due to its ecological sensitivity, fragility, and significant impact received from road development.

The southwest terrain of the Western Sichuan Plateau is higher than the northeast terrain, with an average elevation of more than

Table 1
Land use Markov transition matrix from 2010 to 2020 (km²).

	Farmland	Woodland	Pastureland	Waterbody	Built-up land	Unexploited land	Road land	Total (2010)
Farmland	744	768	851	13	16	7	248	2647
Woodland	835	46,428	19,563	97	24	654	1069	68,670
Pastureland	920	22,202	100,054	509	87	6925	1917	132,614
Waterbody	6	58	293	564	4	112	11	1048
Built-up land	14	13	32	0	10	2	14	85
Unexploited land	6	818	6707	129	1	8984	89	16,734
Road land	29	193	230	3	1	18	1930	2404
Total (2020)	2554	70,480	127,730	1315	143	16,702	5278	224,202

4000 m (Fig. 1b). Consequently, the continental plateau climate in this region has more radiation and precipitation and a larger temperature difference. Its annual average astronomical radiation, precipitation and temperature are 30.217–32.102 MJ/m²/d, 289.252–1111.71 mm, and −14.638–16.187°C, respectively. Since 2010, the land use intensity in the study area has increased. The Markov transition matrix showed that extensive land, including pastureland, woodland, and farmland, has been exploited for road construction (Table 1). The degradation of pastureland and woodland increases ecological risks in the study region. As of 2020, the total expressway, first-class and second-class highway mileages of the study area are 511.679 km, 1293.442 km, and 3106.370 km, respectively. The land used for roads accounts for 2.35 % of the total area (Fig. 1c).

2.2. Ecosystem services assessment within the road-effect zone

The premises of the ecosystem services assessment within the road-effect zone are to evaluate the regional habitat quality, water yield, and soil erosion and to determine the width of the road-effect zone of different road categories. The InVEST approach was utilized to assess regional ecosystem services, which typically quantify ecosystem services and their values on raster maps based on production functions. The case analysis method was employed to determine the width of the road-effect zone of different categories. Then, GIS tools were applied for buffer analysis and extraction by road-effect zone masks to achieve ecosystem service assessment in road-effect zones.

2.2.1. Habitat quality evaluation

The InVEST Habitat Quality module can generate a spatial distribution map of habitat quality by combining current land use and biodiversity threat factors. The process includes calculating the total threat level according to Eq. (1) and then generating the habitat quality map according to Eq. (2).

$$D_{xj} = \sum_{r=1}^R \sum_{y=1}^{Y_r} \frac{w_r}{\sum_{r=1}^R w_r} r_y \beta_x S_{jr} \exp\left(-\frac{2.99}{d_{r\max}} d_{xy}\right) \quad (1)$$

where D_{xj} represents the threat level of the j th land cover's x th grid cell, w_r represents the impact weight of the threat factor r on all habitats, r_y represents the y th grid cell's threat intensity of the threat factor r , d_{xy} represents the linear distance between the x th land cover grid and y th threat grid, $d_{r\max}$ represents the maximum effect distance of the threat factor r , β_x represents the protection level of the x th land cover grid, S_{jr} represents the sensitivity of the j th land cover to the threat r (Zhang et al., 2020).

$$HQ_{xj} = H_j \left(1 - \frac{D_{xj}^z}{D_{xj}^z + k^z}\right) \quad (2)$$

where HQ_{xj} represents the habitat quality of the j th land cover's x th grid cell, H_j represents the habitat suitability of the j th land cover, k represents the scale factor with an initial value of 0.5, and its final value is the maximum threat level of all grid cells (Zhang et al., 2020). The value of Z is 2.5.

In short, the main threats are roads, farmland and built-up land (Zhang et al., 2020), and the impact of roads varies in scope and extent depending on their grade and structure (Wei et al., 2022). Therefore, road threats are further categorized based on road grade and structure, as detailed in Table A1.

2.2.2. Water yield evaluation

The InVEST Water Yield module estimates the water production per grid based on the assumption of Budyko's water-heat coupling balance, that is, precipitation minus the actual evapotranspiration (Sharp et al., 2018) (Eq. (3)).

$$WY(x) = P(x) - AET(x) = \left(1 - \frac{AET(x)}{P(x)}\right) \times P(x) \quad (3)$$

where $AET(x)$ and $P(x)$ represent the annual actual evapotranspiration and precipitation of the x th grid cell, respectively, measured in mm. For land covered by vegetation, such as woodland, pastureland, and farmland, $AET(x)/P(x)$ can be expressed as Eq. (4). For other land without vegetation cover, such as waterbodies, built-up land, unexploited land and road land, $AET(x)$ can be expressed as Eq. (5).

$$\frac{AET(x)}{P(x)} = 1 + \frac{K_c(l_x) \times ET_0(x)}{P(x)} - \left[1 + \left(\frac{K_c(l_x) \times ET_0(x)}{P(x)} \right)^\omega \right]^{1/\omega} \quad (4)$$

$$AET(x) = \min(PET(x), P(x)) = \min(K_c(l_x) \times ET_0(x), P(x)) \quad (5)$$

where ω represents the nonphysical parameters associated with climate and soil properties such as plant available water content (AWC), precipitation and its seasonal distribution (Donohue et al., 2012). $ET_0(x)$ represents the evapotranspiration of the reference crop (i.e., alfalfa) in the x th grid cell and was calculated using the modified Hargreaves function. $K_c(l_x)$ represents the plant (vegetation) evapotranspiration coefficient K_c of the land cover l_x , which can correct the evapotranspiration from the reference crop to the specific vegetation type.

Overall, the road effects on water yield are derived from the differences in the plant (vegetation) evapotranspiration coefficient (i.e., $K_c(l_x)$) and AWC between the road-effect zone and other land covers, with the road structure playing a significant role. Therefore, roadbed sections can be regarded as land without vegetation, and their K_c is between 0.001 and 0.3 (Wang et al., 2023). Bridge sections (crossing rivers) can be regarded as canals, and their K_c is between 0.5 and 1 (Pan et al., 2013). The $K_c(l_x)$ and AWC of bridge sections (crossing over pastures and other nonriver features) and tunnel sections are consistent with the surrounding land cover. The K_c for different land covers is detailed in Table A2.

2.2.3. Soil erosion evaluation

The InVEST Sediment Delivery Ratio module revises the universal soil loss equation to estimate the total annual soil erosion in the grid cells (Eq. (6)).

$$SE = R \times K \times LS \times C \times P \quad (6)$$

where R , K , LS , C , and P represent factors of rainfall erosivity ($\text{MJ}\cdot\text{mm}(\text{ha}\cdot\text{hr})^{-1}$), soil erodibility ($\text{ton}\cdot\text{ha}\cdot\text{hr}(\text{MJ}\cdot\text{ha}\cdot\text{mm})^{-1}$), slope length and gradient, crop management, and support practices, respectively.

R and K were both calculated by the formula proposed by He et al. (2019). LS was obtained by adopting the two-dimensional surface calculation method developed by Desmet and Govers (1996). C refers to the soil erosion ratio between vegetated or crop-managed land and continuous leisure land under the same conditions, ranging from 0 to 1. P refers to the soil erosion ratio of land with and without soil and water conservation measures, ranging from 0 to 1.

The aforementioned factors, such as soil erodibility (K), slope length and gradient (LS), crop management (C), and support practice (P), within the road-effect zone vary across different road structures. Therefore, the K factor needs to be corrected based on engineering surveys and design data, and the values of the C factor and P factor for roadbed sections are 0.2 and 0.9 (Dai et al., 2013; Li et al., 2017; Trisurat et al., 2016), respectively. The impacts of bridge and tunnel sections on topography are relatively small, where K , LS , C , and P are consistent with the surrounding land cover types. The magnitudes of C and P for different land covers are detailed in Table A2.

2.2.4. Road-effect zone determination

Roads vary in engineering and traffic characteristics (i.e., pavement structure and width, designed speed, and traffic volume) among different grades, as well as their road-effect zones (Wei et al., 2022). Internationally, the buffer widths for expressways, first-class and second-class highways are 1 km, 500 m, and 250 m, respectively. In the Chinese specifications for environmental impact assessment and soil and water conservation of highways, the width of the road-effect zone is 60–300 m. Case studies were conducted on road ecology studies, and the results showed that the road-effect zones of different grades of roads to species (e.g., birds, large mammals) ranged from 250 m to 5 km (Asadolahi et al., 2018; Benitez-Lopez et al., 2010; Terrado et al., 2016; Wu et al., 2014), and the commonly used road-effect zones in studies were from 300 m to 5 km (Bao et al., 2015; Gong et al., 2018; Wang et al., 2016; Wu et al., 2021; Zhang et al., 2016). Hence, considering that the resolution of raster data is 1 km, the road-effect zones of the roadbed sections of expressways, first-class and second-class highways on habitat quality are 4 km, 3 km, and 2 km, respectively, and their road-effect zones on water yield and soil erosion are both 1 km. The road-effect zones of all bridge and tunnel sections are both 1 km.

2.3. Impact analysis

The ecosystem service changes within the road-effect zone are related to road attributes (i.e., road grade, structure, length, and operation duration), natural climate, geographic location, topography, soil properties, land cover, and so on.

Specifically, for habitat quality assessment, from the production functions of Eqs. (1) and (2), the data needed include land cover raster maps, raster maps depicting the spatial distribution of threats, the vector of the nature reserve, and parameters such as threat weights, maximum effect distance, habitat sensitivities, and habitat suitability. Among these, changes in land cover and the intensity of spatial threat distribution (related to road grade, structure, length, distance from the road centerline, and operation duration) are frequent and closely associated with habitat quality changes.

For water yield assessment, from the production functions of Eqs. (3)–(5), the necessary data comprise several raster maps, including annual mean precipitation, plant available water content (AWC), astronomical radiation, annual average daily maximum and minimum temperature, and land cover, as well as the vector of the watersheds and vegetation evapotranspiration coefficient (K_c). Among these, changes in precipitation, temperature, AWC (related to road structure, length, and operation duration), astronomical radiation (related to latitude), and K_c (related to land cover and road structure) are frequent and closely associated with water yield

Table 2
Presentation of the influencing factors.

Influencing factor	Denotation	Value
Road structure	<i>T</i>	0: roadbed section 1: tunnel section 2: bridge section
Road grade	<i>C</i>	0: expressway 1: first-class highway 2: second-class highway
Land cover change	<i>U</i>	17: farmland being exploited for road use 27: woodland being exploited for road use 37: pastureland being exploited for road use 47: waterbody being exploited for road use 57: built-up land being exploited for road use 67: unexploited land being exploited for road use 77: no change
Road length (km)	<i>L</i>	decimal
Road operation duration (as of 2020)	<i>Y</i>	decimal
Distance from the road centerline (m)	<i>D</i>	decimal
Precipitation change (mm)	<i>P</i>	decimal
Annual average temperature change (°C)	<i>TE</i>	decimal
Plant available water content (mm)	<i>AWC</i>	decimal
Latitude (°)	<i>LA</i>	decimal
Elevation (m)	<i>H</i>	decimal
Changes in soil erodibility factors (ton·ha·hr(MJ·ha·mm) ⁻¹)	<i>KC</i>	decimal

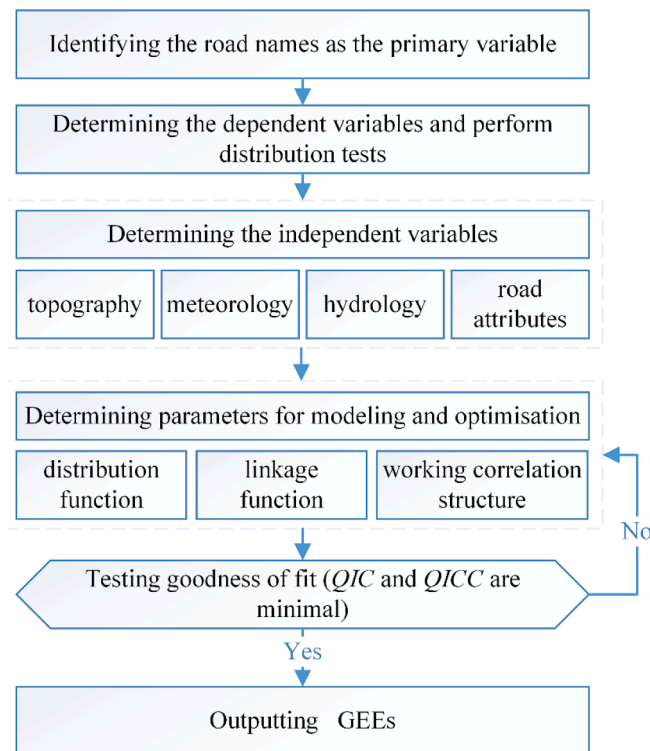


Fig. 2. The establishment and optimization process of GEEs.

changes.

Furthermore, for soil erosion assessment, from the production functions of Eq. (6), the data needed include several raster maps, such as land cover, monthly precipitation, annual mean precipitation, and elevation, as well as the vector of the watersheds, soil types, and parameters such as crop management and support practices. Among them, changes in land cover, precipitation, elevation, soil types (affecting soil erodibility factors and being related to road structure and length), and crop management and support practices (related to road structure, length, and operation duration) are frequent and closely associated with soil erosion changes.

In summary, the data needed for ecosystem service assessment and their interpretation and sources are outlined in Table A3. The

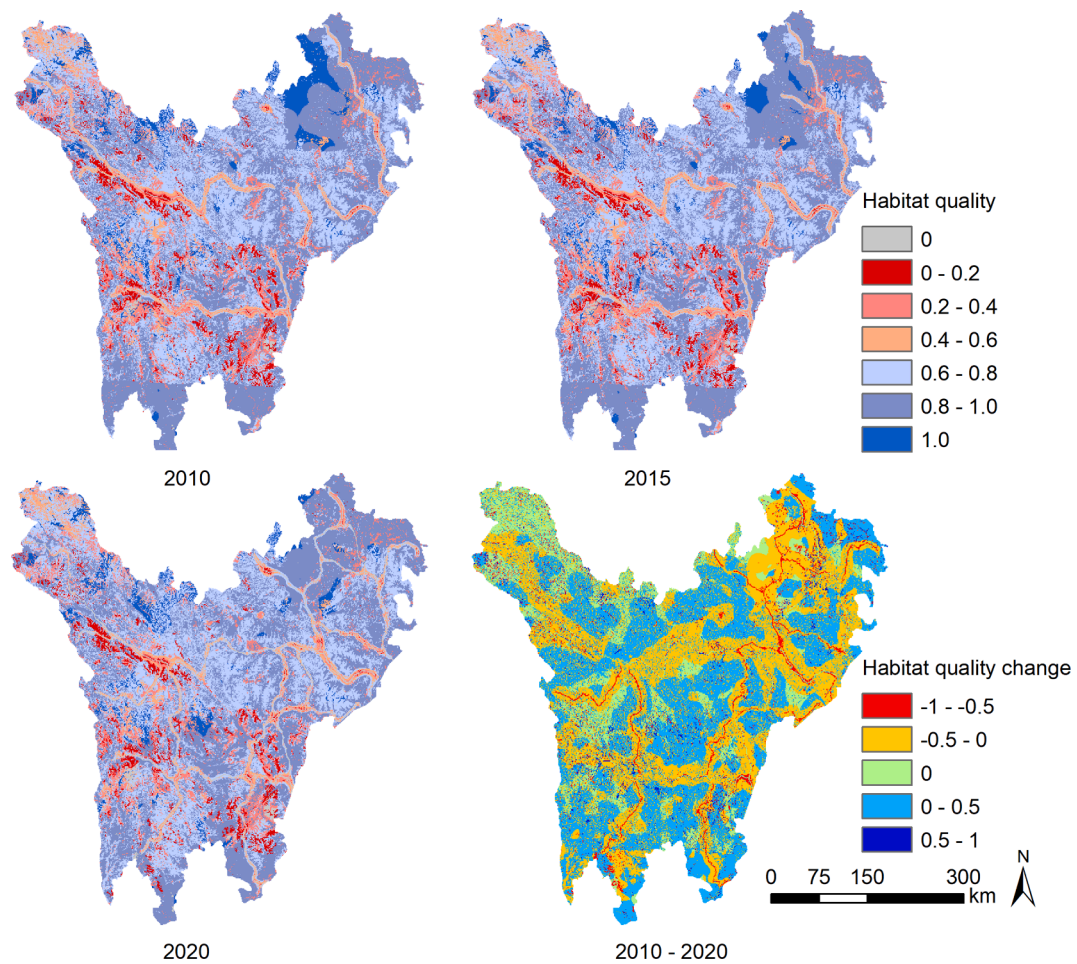


Fig. 3. Spatiotemporal distribution and changes in habitat quality in the study region from 2010 to 2020.

influencing factors and their values identified in the impact analysis of ecosystem service changes within the road-effect zone are presented in Table 2.

The influencing factors (independent variables) and ecosystem service changes (dependent variables) include continuous and categorical variables, and the dependent variables may display different distribution patterns. In addition, a road will provide data points at multiple locations, which may be correlated. Therefore, this study took each road as the primary variable and introduced GEEs to model geographic data such as influencing factors and ecosystem service changes.

The establishment and optimization process of GEEs is shown in Fig. 2, which determines the optimal working correlation structure and models according to the quasi-likelihood under independence model criterion (QIC) and the corrected quasi-likelihood under independence model criterion (QICC) (Abbasi and Keshavarzi, 2019; Kwon et al., 2017).

3. Results and discussion

3.1. Road-effect zone ecosystem services

3.1.1. Habitat quality

The spatiotemporal distribution of habitat quality in the study region was not uniform (Fig. 3), and the overall average habitat quality decreased from 0.752 in 2010 to 0.738 in 2020. The annual average habitat quality and its changes within the road-effect zone are shown in Fig. 4, and the results showed that the habitat quality in the road-effect zone and the study region both showed a downward trend, but the former decreased more obviously. Specifically, the average habitat quality of expressways and first-class and second-class highways declined from 0.574, 0.464, and 0.62 in 2010 to 0.389, 0.445, and 0.384 in 2020, respectively, among which the average habitat quality within the second-class highways decreased the most (with a decline ranging from 0 to 0.4), followed by expressways (with a decline ranging from 0.2 to 0.5) and first-class highways (with a decline ranging from 0 to 0.3). Furthermore, the highest average decrease in habitat quality occurred within the roadbed sections, followed by the bridge sections and tunnel sections.

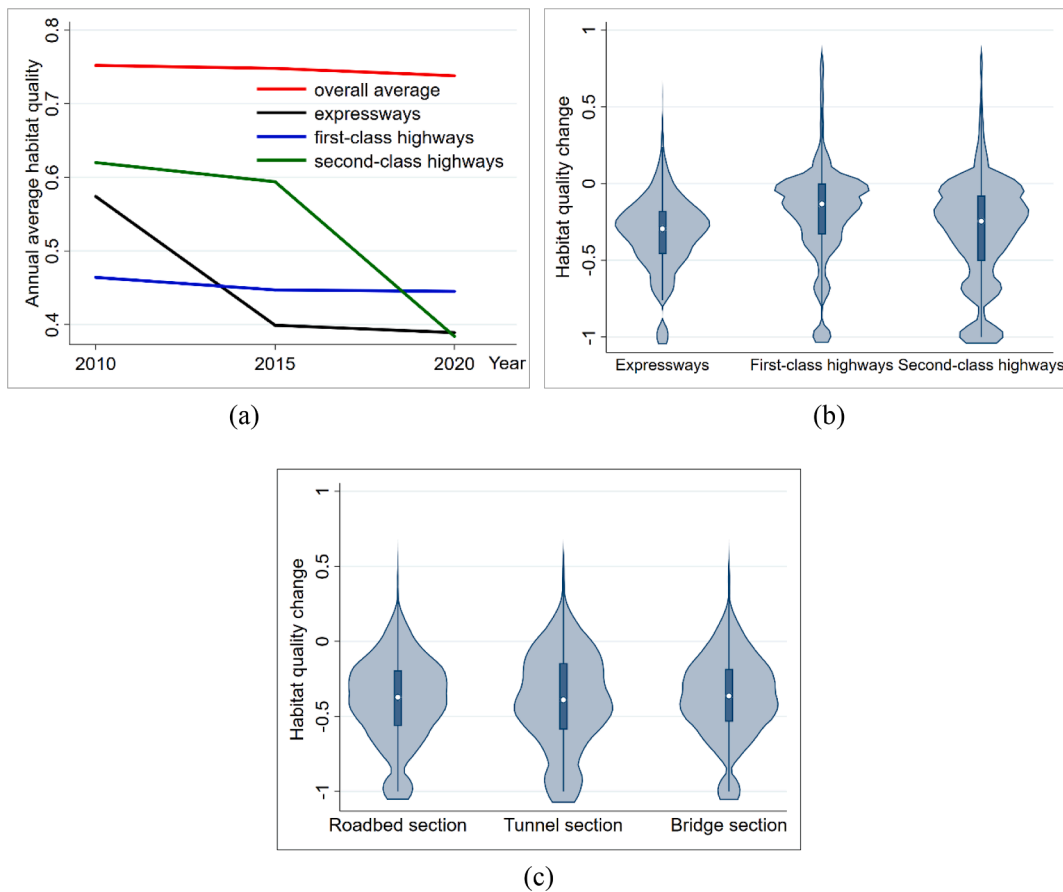


Fig. 4. The annual average habitat quality (a) and distribution of habitat quality changes for different grades (b) and structures (c) of roads.

The results indicate that the roadbed sections of high-grade highways have the most severe impact on habitat quality, possibly due to their wider cross sections and fully enclosed forms, which reduce habitat connectivity and increase landscape fragmentation (Wei et al., 2022; Zhang et al., 2020). Despite the narrower and more open cross sections of second-class highways, they exhibit higher negative impacts on habitat quality in the study due to their longer mileage and susceptibility to wildlife injuries and fatalities (Llagostera et al., 2022).

3.1.2. Water yield

The annual water yield in the study region showed an obvious horizontal distribution, with an increasing trend from west to east (Fig. 5). The overall annual average water yield decreased from 879.983 mm in 2010 to 687.775 mm in 2020, which was consistent with the water yield calculated by Wei et al. (2021) in northwestern Yunnan and by Yu et al. (2022) in the northeastern QTP. The annual average water yield and its changes within the road-effect zone are shown in Fig. 6, and the results indicated that the fluctuating trend of the annual average water yield within the road-effect zone was consistent with that in the study region, first decreasing and then slightly increasing, showing an overall downward trend. Clearly, the annual average water yield in the road-effect zone was higher than that in the study region. In addition, expressways had the greatest negative impact on water yield (with a decline ranging from 200 to 300 mm), followed by second-class highways (with a decline ranging from 100 to 300 mm) and first-class highways (with a decline ranging from 0 to 200 mm). The rise in precipitation led to an increase in water yield of approximately 50 mm in certain first-class highways. Furthermore, the most substantial average decrease in water yield occurred within the tunnel sections, followed by bridge sections and roadbed sections.

The results indicate that changes in climate and land cover have a significant impact on water yield, with precipitation changes contributing the most. This is consistent with the findings of Wang et al. (2023) and Yang et al. (2020). The occupation of pastureland and woodland by additional highways results in reduced water yield, potentially explaining the greater decrease in water yield within the road-effect zones of wider expressways and longer second-class highways. Therefore, it is recommended to prioritize the use of unexploited land during road planning. Additionally, densely vegetated tunnel sections experience the most substantial reduction in water yield due to higher vegetation evapotranspiration coefficients and potential evapotranspiration, while the opposite is true for bridge and roadbed sections. Groundwater drawdown caused by tunnel drainage may also have far-reaching impacts on hydrology, ecology and the environment (Lv et al., 2020).

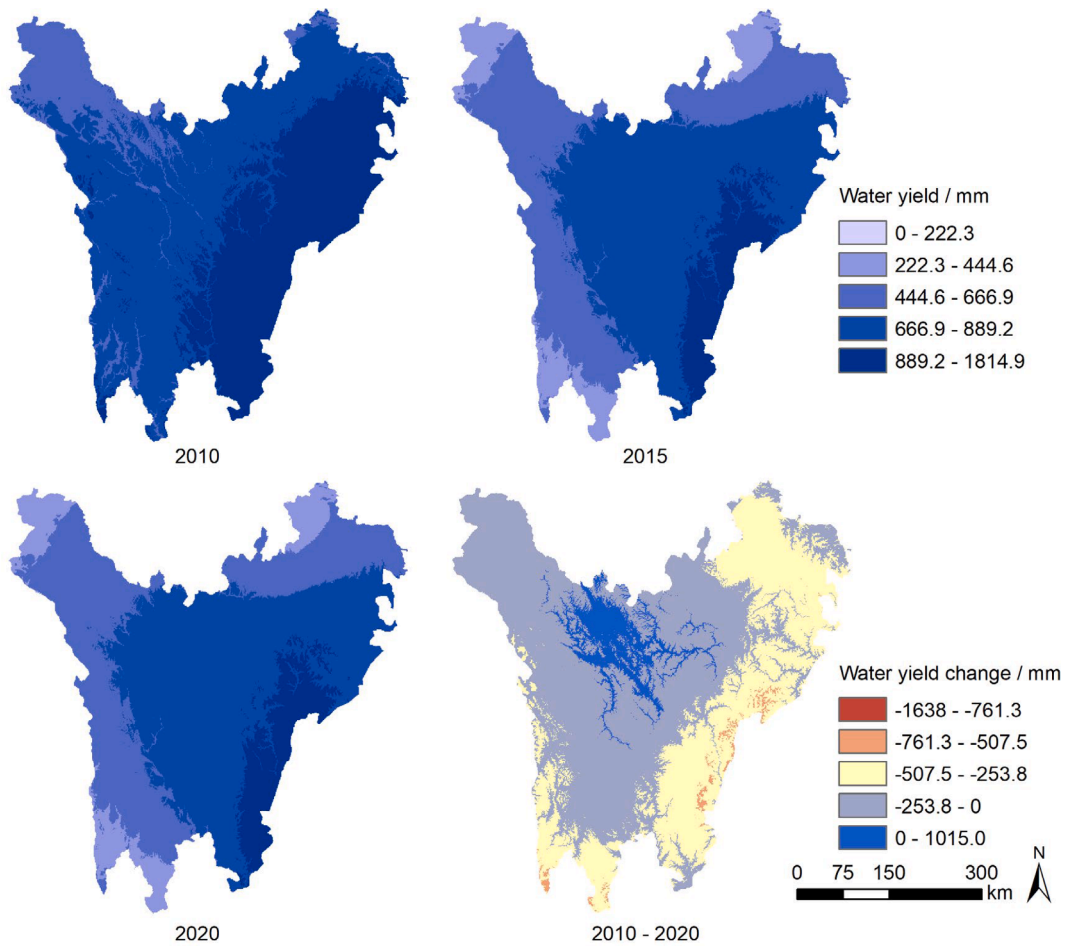


Fig. 5. Spatiotemporal distribution and changes in water yield in the study region from 2010 to 2020.

3.1.3. Soil erosion

The spatiotemporal distribution of soil erosion in the study region was also uneven (Fig. 7). The overall annual average soil erosion decreased from $187.59 \text{ t}\cdot\text{ha}^{-1}$ in 2010 to $117.68 \text{ t}\cdot\text{ha}^{-1}$ in 2020, which was consistent with the soil erosion calculated by Ran et al. (2020) in northwestern China. The annual average soil erosion and its changes within the road-effect zone are shown in Fig. 8, and the results showed that the annual average soil erosion within the road-effect zone was on the rise, which was opposite to that in the study region. The annual average soil erosion within the expressways was the highest, followed by second-class highways and first-class highways, with a similar pattern of change in soil erosion within the road-effect zones (with a range from -2.5 to $5 \text{ t}\cdot\text{ha}^{-1}$). Furthermore, the highest average increase in soil erosion occurred within the bridge sections, followed by roadbed sections and tunnel sections.

The results indicate that precipitation and slope are the primary contributors to changes in soil erosion, which is consistent with the findings of Guo et al. (2023) and Matomela et al. (2022). Expressways and second-class highways are mainly located in the eastern part of the study region, with abundant rainfall and higher rainfall erosivity, leading to a greater increase in soil erosion. Additionally, extensive slope excavation and vegetation destruction along expressways also contribute to increased soil erosion (Hacisalihoglu et al., 2019). Therefore, comprehensive slope management should be emphasized, and a combination of plant-based and engineering measures should be implemented to preserve soil and water along slopes of highways. Furthermore, inspections should be intensified, and drivers should be reminded to prioritize traffic safety during the rainy season (Li et al., 2019). The relatively minor change in soil erosion in the tunnel sections is attributed to the disruption of the topography and geomorphology only at the tunnel opening. Conversely, the construction of bridge piers in bridge sections can alter certain soil properties and increase soil erodibility, potentially leading to streambank erosion.

3.2. Analysis of the ecosystem services reduction factors

3.2.1. GEE for habitat quality change

Taking road structure (T), road grade (C), land cover change (U), road length (L), road operation duration (Y), and distance from

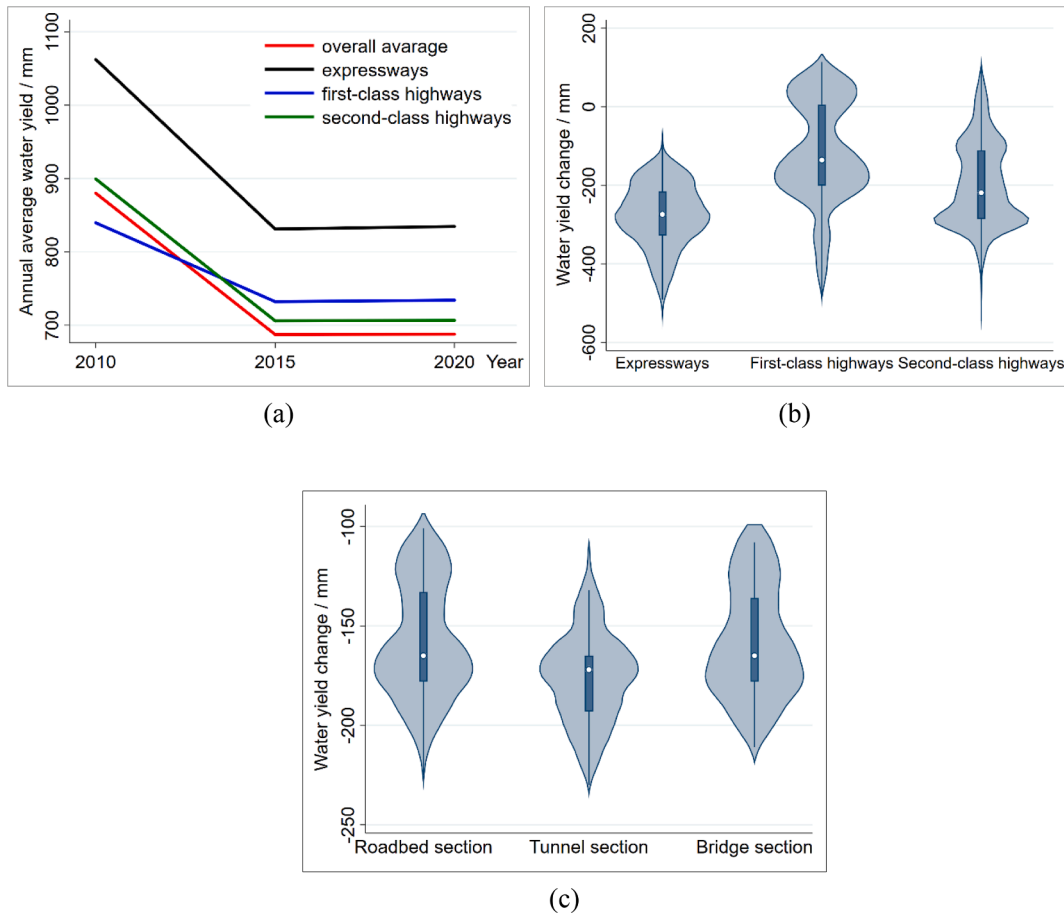


Fig. 6. The annual average water yield (a) and distribution of water yield changes for different grades (b) and structures (c) of roads.

the road centerline (D) as independent variables, the habitat quality changes (HQC) within the road-effect zone was the dependent variable, and GEE for habitat quality was formulated. The frequency distribution histogram and Q-Q plot in Fig. 9 and the results of the skewness/kurtosis test of the dependent variable (P value less than 0.05) all indicated that the HQC sample does not follow the normal distribution. Therefore, the probability distribution, linkage function, and working correlation structure of the GEE were set as the binomial distribution, logit function, and independent variables, respectively.

The GEE modeling results in Table 3 show that compared with first-class highways, both expressways and second-class highways reduced the habitat quality within the road-effect zone ($B < 0$), and their negative effects were similar. Compared with roadbed sections, the bridge and tunnel sections improved the habitat quality within the road-effect zone ($B > 0$), and the habitat quality of the tunnel sections was higher. The habitat quality improved with increasing land cover change ($B = 0.047$), indicating that developing unexploited land for road construction can reduce the negative impact on habitat quality. Similarly, the habitat quality improved with the increase in the road operation duration ($B = 0.324$) and the distance from a road centerline ($B > 0$), indicating that the road had the greatest negative impact on the habitat quality during the construction and initial operation stages, and then tended to stabilize and improv. In addition, the effect of road length on habitat quality was not significant (P value = 0.714).

3.2.2. GEE for water yield change

Taking road structure (T), land cover change (U), road length (L), road operation duration (Y), precipitation change (P), annual average temperature change (TE), plant available water content (AWC), and latitude (LA) as independent variables, the water yield changes (WYC) within the road-effect zone was the dependent variable, and GEE for water yield was established. The kurtosis and skewness of WYC were 2.250 and 0.270, respectively, and their frequency distribution histogram and Q-Q plot are shown in Fig. 10, indicating that the WYC sample does not follow the normal distribution. Therefore, the probability distribution, linkage function, and working correlation structure of the GEE were set as the binomial distribution, logit function, and independent variables, respectively.

The GEE modeling results in Table 4 show that compared with tunnel sections, both roadbed and bridge sections increased the water yield within the road-effect zone ($B > 0$), and the impact of the two was similar. The main reason was that the plant evapotranspiration coefficient of roadbed sections was lower, and bridge sections were easily identified as roadbed sections with a grid resolution of 1 km. With the rise in precipitation ($B = 1.004$), the decrease in temperature ($B = -1.259$), and the increase in AWC ($B =$

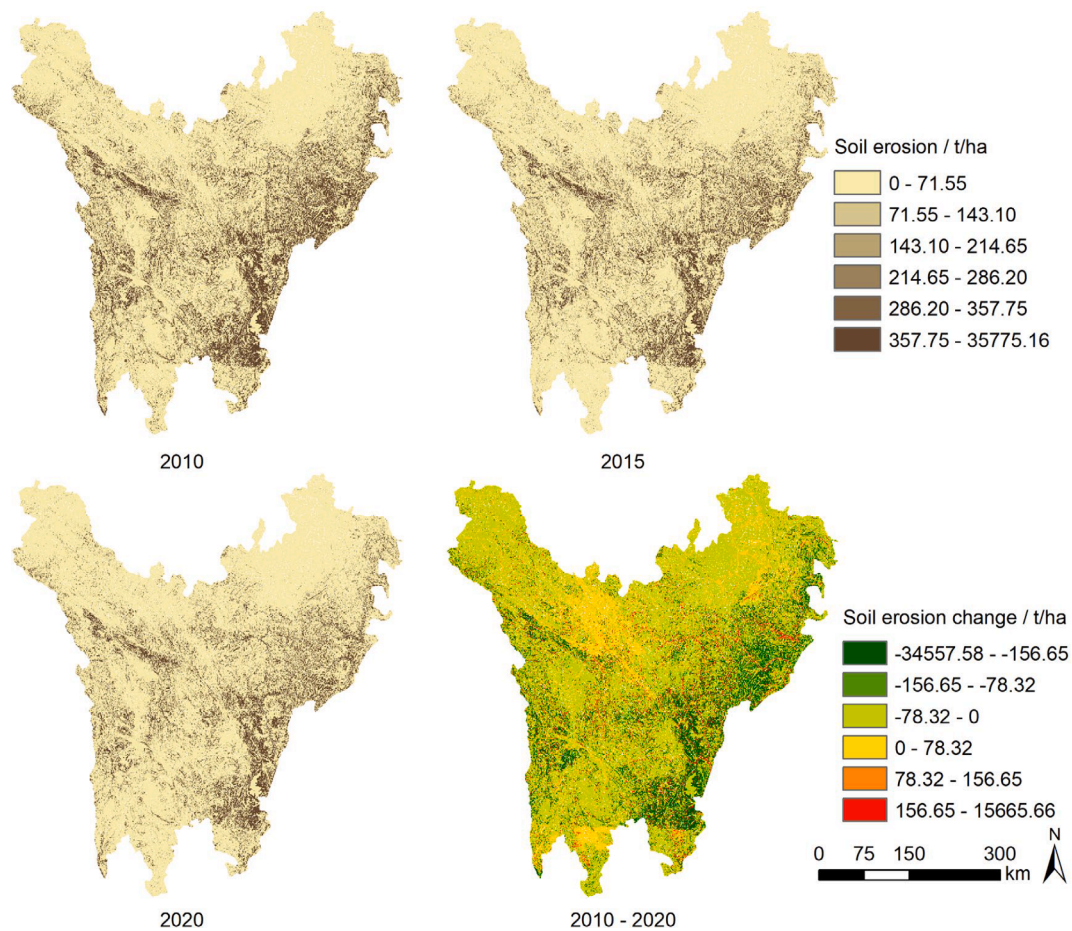


Fig. 7. Spatiotemporal distribution and changes in soil erosion in the study region from 2010 to 2020.

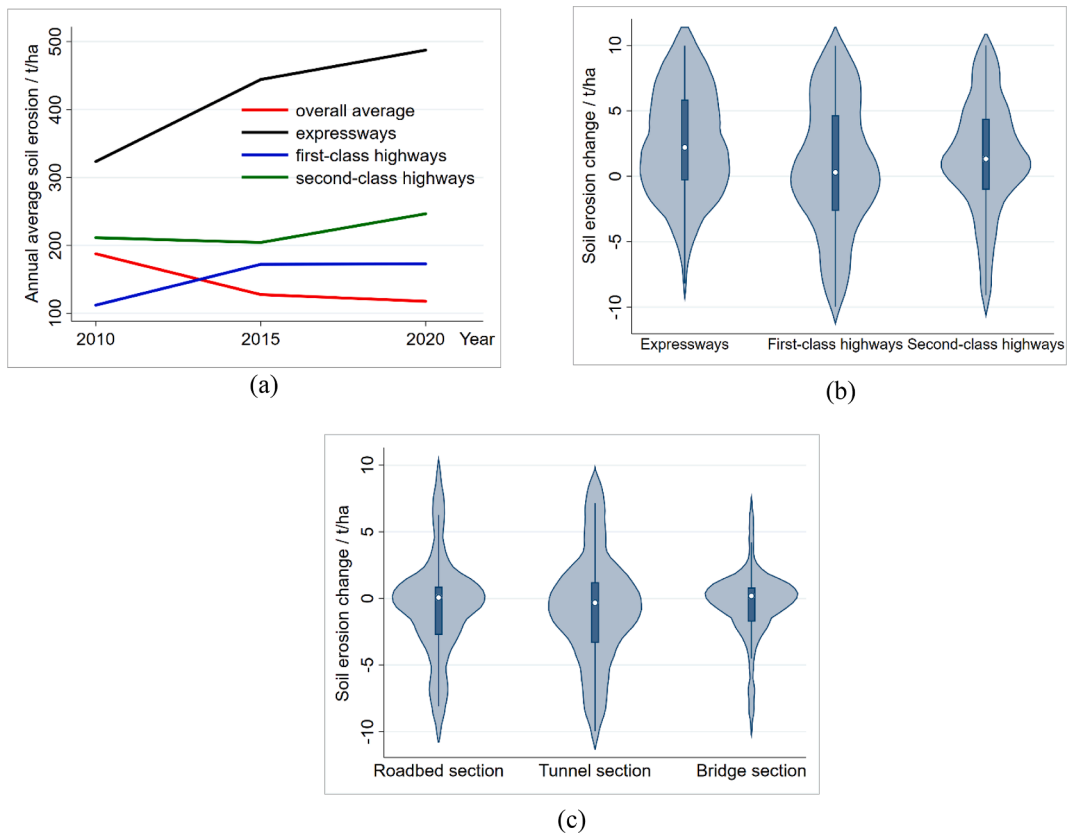


Fig. 8. The annual average soil erosion (a) and distribution of soil erosion changes for different grades (b) and structures (c) of roads.

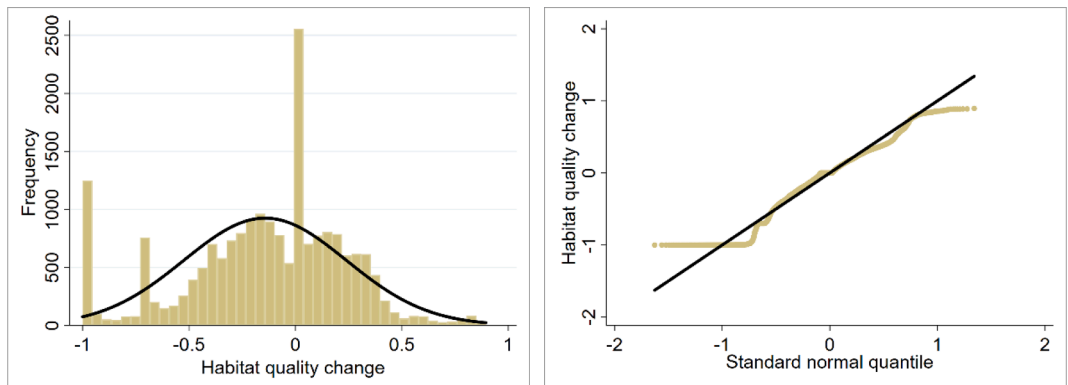


Fig. 9. Frequency distribution histogram (left) and Q-Q plot (right) of HQC.

0.008), the water yield within the road-effect zone increased ($B > 0$). The water yield increased with the increasing land use change ($B = 0.018$), indicating that developing unexploited land for road construction can reduce the negative impact on water yield. Similarly, the water yield decreased with increasing road operation duration ($B = -0.097$) and road length ($B < 0$), indicating that the negative impact of roads on the water yield became more severe. In addition, the effect of latitude on water yield was not significant (P value = 0.117).

3.2.3. GEE for soil erosion change

Taking road structure (T), road length (L), road operation duration (Y), land cover change (U), precipitation change (P), elevation (H), and change in soil erodibility factors (KC) as independent variables, the soil erosion change (SEC) within the road-effect zone was the dependent variable, and the GEE for soil erosion was established. The kurtosis and skewness of SEC were 2.671 and -0.261 , respectively, and their frequency distribution histogram and Q-Q plot are shown in Fig. 11, indicating that the SEC sample does not

Table 3
GEE modeling results (habitat quality change within the road-effect zone).

Parameters	Estimated coefficient (<i>B</i>)	Standard error	95 % Wald confident interval		<i>P</i> value
			Lower	Upper	
Intercept	-4.722	0.782	-6.255	-3.190	0
T_0 = Roadbed section	control group				
T_1 = Tunnel section	1.950	0.728	0.524	3.377	0.007
T_2 = Bridge section	0.649	0.730	-0.781	2.078	0.374
C_0 = Expressway	-1.203	0.521	-2.224	-0.183	0.021
C_1 = First-class highway	control group				
C_2 = Second-class highway	-1.349	0.354	-2.043	-0.655	0
Land cover change (<i>U</i>)	0.047	0.006	0.036	0.058	0
Road length (<i>L</i>)	0	0	0	0	0.714
Road operation duration (<i>Y</i>)	0.324	0.038	0.249	0.399	0
Distance from the road centerline (<i>D</i>)	0	0	0	0.001	0
Goodness of fit	QIC = 14854.576; QICC = 14275.831				

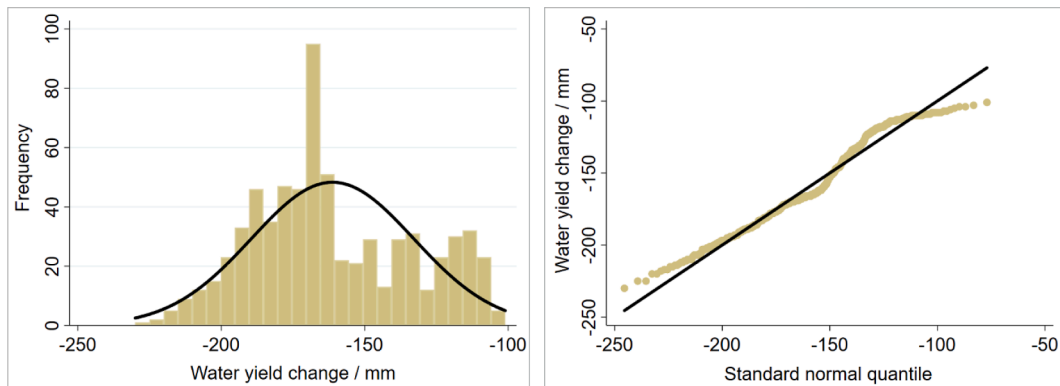


Fig. 10. Frequency distribution histogram (left) and Q-Q plot (right) of WYC.

Table 4
GEE modeling results (water yield change within the road-effect zone).

Parameters	Estimated coefficient (<i>B</i>)	Standard error	95 % Wald confident interval		<i>P</i> value
			Lower	Upper	
Intercept	-4.217	4.994	-14.006	5.571	0.398
T_0 = Roadbed section	2.648	0.934	0.816	4.479	0.005
T_1 = Tunnel section	control group				
T_2 = Bridge section	2.654	0.062	2.534	2.775	0
Precipitation change (<i>P</i>)	1.004	0.001	1.002	1.007	0
Annual average temperature change (<i>TE</i>)	-1.259	0.459	0.360	2.158	0.006
Plant available water content (<i>AWC</i>)	0.008	0.003	0.001	0.014	0.020
Land cover change (<i>U</i>)	0.018	0.010	-0.002	0.038	0.076
Road length (<i>L</i>)	0	0	0	0	0.004
Road operation duration (<i>Y</i>)	-0.097	0.032	-0.160	-0.034	0.003
Latitude (<i>LA</i>)	0.239	0.152	-0.060	0.537	0.117
Goodness of fit	QIC = 1393361.804; QICC = 1393341.940				

follow the normal distribution. Therefore, the probability distribution, linkage function, and working correlation structure of the GEE were set as the binomial distribution, logit function, and independent variables, respectively.

The GEE modeling results in Table 5 indicated that compared with roadbed sections, tunnel sections reduced soil erosion within the road-effect zone ($B = -1.466$), while bridge sections increased soil erosion within the road-effect zone ($B = 0.545$) because the damage to the vegetation and soil in the tunnel sections is slight, while the bridge sections could erode river banks and soil. With the increase in soil erodibility factors ($B = 50.719$) and precipitation ($B = 0.002$) and the decrease in land cover change ($B = -0.047$) and elevation ($B < 0$), the soil erosion within the road-effect zone rose. Soil erosion decreased with increasing road operation duration ($B = -0.028$) and distance from the road centerline ($B < 0$) as soil erodibility declined. However, the effects of road operation duration and the distance from a road centerline were not significant (P value > 0.05).

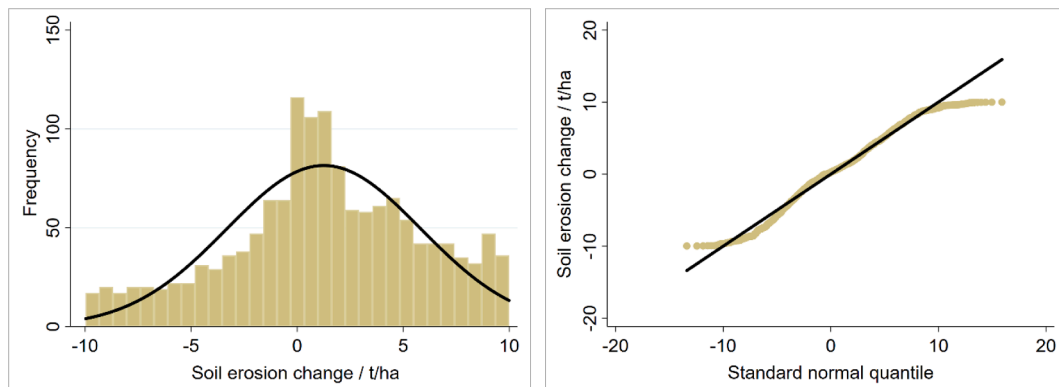


Fig. 11. Frequency distribution histogram (left) and Q-Q plot (right) of SEC.

Table 5
GEE modeling results (soil erosion change within the road-effect zone).

Parameters	Estimated coefficient (B)	Standard error	95 % Wald confident interval		P value
			Lower	Upper	
Intercept	0.897	0.303	0.303	1.491	0.003
T_0 = Roadbed section	control group				
T_1 = Tunnel section	-1.466	0.047	-1.558	-1.374	0
T_2 = Bridge section	0.545	0.060	0.427	0.663	0
Change in soil erodibility factors (KC)	50.719	5.635	39.674	61.764	0
Elevation (H)	0	0	0	0	0
Precipitation change (P)	0.002	0.001	0.001	0.003	0
Land cover change (U)	-0.047	0.004	-0.056	-0.039	0
Road length (L)	0	0	0	0	0.281
Road operation duration (Y)	-0.028	0.015	-0.057	0.001	0.054
Goodness of fit	QIC = 7316.948; QICC = 7296.785				

4. Conclusions

This study assessed the spatiotemporal distribution of ecosystem services in road-effect zones and explored the synergistic impacts among road attributes and natural factors to ecosystem service changes. The primary contribution of this study is to extend the application of the INVEST and GEEs approaches to the field of road engineering, providing a promising method for quantitatively assessing and predicting the impact of roads on ecology. A case study was conducted to validate and examine the proposed approach, yielding the following primary conclusions.

- (1) The habitat quality within the road-effect zones is mostly affected by road grade and structure. Roadbed sections of expressways and second-class highways have the greatest negative impact on habitat quality, followed by roadbed sections of first-class highways and bridge and tunnel sections of highways. Improving the road grade class and extending the road length may also reduce habitat quality. Hence, in the planning and design of high-grade highways, it is essential to reserve adequate and well-located wildlife crossings to enhance habitat connectivity. In the case of low-grade roads, given their limited enclosure, in addition to access design, traffic signs should be strategically placed at key intersections to prompt drivers to slow, thereby minimizing the risk of injuring crossing wildlife.
- (2) Reduced precipitation, increased temperature, decreased AWC and the comprehensive effect of road structure and operation duration are significant influences in reducing water yield within the road-effect zones. The tunnel sections have the lowest water yield, followed by roadbed sections and bridge sections, as reflected by the AWC and vegetation evapotranspiration coefficient. Furthermore, the longer the road has been in operation, the lower the water yield. Therefore, it is essential to focus on the long-term soil and water erosion of the road and ensure proper maintenance of the slopes.
- (3) Higher soil erodibility factors, precipitation, and road structure are significant factors that increase soil erosion within the road-effect zone. The soil erosion in the bridge sections is the most serious, followed by roadbed and tunnel sections. Furthermore, soil erosion is more severe in high-grade highways. This is due to the inconsistent extent of damage to the ground surface of roads with different grades and structures. Therefore, in the construction and operation of roads, it is important not only to

Table A1
Threat features.

Threats	Weight	Maximum effect distance (km)	References
Farmland	0.8	4	(Shaffer et al., 2019; Terrado et al., 2016; Wu et al., 2014)
Built-up land	1	5	
Roadbed sections of expressways	0.9–1	4	(Hu et al., 2018; Li et al., 2019; Wu et al., 2014; Zhang et al., 2020)
Roadbed sections of first-class highways	0.8–0.9	3	
Roadbed sections of second-class highways	0.7–0.8	2	
Bridge and tunnel sections of all roads	0.2–0.3	1	

Table A2
 K_c , C and P factors for different land covers.

Land cover	K_c	C	P
Paddy field	0.65	0.18	0.4
Dry land	0.6	0.23	0.4
Woodland	1	0.004	1
Shrub	1	0.06	1
Sparse woodland	0.85	0.08	1
Other woodland	0.75	0.1	0.2
High coverage pastureland	0.85	0.043	1
Medium coverage pastureland	0.75	0.15	1
Low coverage pastureland	0.65	0.45	1
River channel	1	0	0
Lake	1	0	0
Reservoir pit	1	0	0
Permanent glacier snow	0.5	0	0
Tidal flat	1	0.18	0.4
Beach	1	0	0
Urban land	0.2	0.2	1
Rural settlement	0.3	0.2	1
Other construction land	0.1	0.2	1
Sandy land	0.2	1	1
Gobi	0.2	1	1
Saline-alkali land	0.2	1	1
Wetlands	1	0	1
Bare land	0.3	1	1
Bare rock texture	0.2	1	1
Other exploited land	0.5	1	1
Roadbed sections	0.1	0.2	0.9
Bridge sections (crossing rivers)	1	/	/

consider the impact of the main project on soil erosion but also to focus on soil erosion in areas such as soil extraction and disposal sites, construction roads, and other related areas.

In short, ecosystem services are likely to be subjected to roadbed sections and high grades. Hence, it is recommended to reasonably plan road grades and structures, for instance, using bridges or tunnels instead of deep excavation or high filling to pass through ecologically sensitive areas, to achieve sustainable development of linear transportation infrastructure. This study elucidates road ecological restoration, low-environmental-impact route layout, and route scheme comparison. However, it still has some limitations. First, limited by the lower resolution of the raster map, the road attributes in this study only include road grade, structure, length, and operational time. Moreover, there may be errors in distinguishing between tunnels, bridges, and roadbed sections of shorter lengths (<1 km), especially when bridges and tunnels are adjacent. We would like to explore the impact of road geometry design on landscape and ecology by using higher resolution data. Second, due to challenges in obtaining road structure data and the limited availability of tunnels and bridges for lower-grade roads, a few lower-grade roads have not been classified into structural sections but were treated as a whole roadbed section. To overcome limitations in data volume and accuracy, we aim to develop image recognition techniques for the automated and intelligent acquisition of road structures and geometric designs in future work. Furthermore, some of the parameter values in this study have been determined and corrected through literature reviews, such as threat features, road-effect zone width, vegetation evapotranspiration coefficient, and the value of crop management and support practices. While these parameter values have been tested with actual cases and are highly reliable, the most accurate values can be obtained through practical observation and experimentation where possible.

Table A3

Data or parameters needed for ecosystem services assessment and their interpretation and sources.

	Data/parameters	Types	Interpretation	Potential sources (bolding indicates sources for this study)
Habitat quality	Land cover	Raster maps	Including farmland, woodland, pastureland, waterbody, built-up land, unexploited land, and road land	Government or planning agencies, remote sensing interpretation, and specialized scientific research institutes
	Spatial distribution of threats	Raster maps	Including farmland, built-up land, and road land of different grades and structure	Land cover , remote sensing interpretation, and OpenStreetMap (https://www.openstreetmap.org/)
	Nature reserve	Vector maps (polygon features)	Including nature reserves established by national and local authorities at all levels	Government or planning agencies
	Threat weights	Decimal (no unit)	The impact weight of the threat factor on all habitats	Literature review , expert interview or questionnaire survey, and field surveys
	Maximum effect distance of threats	Decimal (unit km)	The maximum effect distance of the threat factor	Literature review , expert interview or questionnaire survey, and field surveys
	Habitat sensitivities	Decimal (no unit)	The sensitivity of each land cover to each threat	Literature review , expert interview or questionnaire survey, and field surveys
	Habitat suitability	Decimal (no unit)	The habitat suitability of each land cover	Literature review , expert interview or questionnaire survey, and field surveys
Water yield	Land cover	Raster maps	Including farmland, woodland, pastureland, waterbody, built-up land, unexploited land, and road land	Government or planning agencies, remote sensing interpretation, and specialized scientific research institutes
	Annual mean precipitation	Raster maps	Total precipitation per year	Meteorological monitoring department, remote sensing interpretation, and specialized scientific research institutes
	Plant available water content (AWC)	Raster maps	Related to plant available water content, maximum root depth of the soil, and depth of plant roots; influenced by road structure, length, and operation duration	Field surveys , and World soil database (HWSD)
	Astronomical radiation	Raster maps	Related to latitude	Numerical calculation
	Annual average daily maximum temperature	Raster maps	Annual average daily maximum temperature	Meteorological monitoring department, remote sensing interpretation, and specialized scientific research institutes
	Annual average daily minimum temperature	Raster maps	Annual average daily minimum temperature	Meteorological monitoring department, remote sensing interpretation, and specialized scientific research institutes
	Watersheds	Vector maps (polygon features)	The spatial distribution of first-class rivers such as the Yangtze River, Yellow River, and Heilongjiang River	Government or planning agencies, remote sensing interpretation, and specialized scientific research institutes
	Vegetation evapotranspiration coefficient (K_e)	Decimal (no unit)	Related to land cover; influenced by road structure	Literature review , expert interview or questionnaire survey, and field surveys

(continued on next page)

Table A3 (continued)

	Data/parameters	Types	Interpretation	Potential sources (bolding indicates sources for this study)
Soil erosion	Land cover	Raster maps	Including farmland, woodland, pastureland, waterbody, built-up land, unexploited land, and road land	Government or planning agencies, remote sensing interpretation, and specialized scientific research institutes
	Monthly precipitation	Raster maps	Total precipitation per month	Meteorological monitoring department, remote sensing interpretation, and specialized scientific research institutes
	Annual mean precipitation	Raster maps	Total precipitation per year	Meteorological monitoring department, remote sensing interpretation, and specialized scientific research institutes
	Elevation	Raster maps	The height or distance above a particular level, especially above sea level	Field surveys, remote sensing interpretation, and specialized scientific research institutes
	Watersheds	Vector maps (polygon features)	The spatial distribution of first-class rivers such as the Yangtze River, Yellow River, and Heilongjiang River	Government or planning agencies, remote sensing interpretation, and specialized scientific research institutes
	Soil types	Raster maps	Related to the content of sand, silt, clay and organic carbon in the soil; influenced by road structure, length, and operation duration	Field surveys , and World soil database (HWSD)
	Crop management	Decimal (no unit)	The soil erosion ratio between vegetated or crop-managed land and continuous leisure land under the same conditions, ranging from 0 to 1	Literature review , expert interview or questionnaire survey, and field surveys
	Support practice	Decimal (no unit)	The soil erosion ratio of land with and without soil and water conservation measures, ranging from 0 to 1	Literature review , expert interview or questionnaire survey, and field surveys

CRediT authorship contribution statement

Hong Zhang: Conceptualization, Funding acquisition, Methodology, Software, Writing – original draft, Writing – review & editing. **Xin Xu:** Formal analysis, Validation, Writing – original draft, Writing – review & editing. **Chi Zhang:** Methodology, Supervision, Writing – review & editing. **Zhi-Peng Fu:** Funding acquisition, Resources, Validation. **Hong-Zhi Yang:** Data curation, Resources, Supervision.

Declaration of competing interest

The authors declare that they have no known competing financial interests or personal relationships that could have appeared to influence the work reported in this paper.

Data availability

Data will be made available on request.

Acknowledgments

This research was funded by the National Key Research & Development Program of China (2021YFB2600103), Inner Mongolia University Young Academic Talent Research Initiation Project (10000-23112101/068), and National Natural Science Foundation of China (72161032). The authors thank the Data Center for Resources and Environmental Science of Chinese Academy of Sciences for providing raster maps of the land use, elevation, precipitation, etc.

Appendix A

See [Tables A1–A3](#).

References

- Abbasi, S., Keshavarzi, B., 2019. Source identification of total petroleum hydrocarbons and polycyclic aromatic hydrocarbons in PM10 and street dust of a hot spot for petrochemical production: Asaluyeh County, Iran. *Sustain Cities Soc.* 45, 214–230. <https://doi.org/10.1016/j.scs.2018.11.015>.
- Ahammad, R., Stacey, N., Eddy, I.M.S., Tomscha, S.A., Sunderland, T.C.H., 2019. Recent trends of forest cover change and ecosystem services in eastern upland region of Bangladesh. *Sci. Total Environ.* 647, 379–389. <https://doi.org/10.1016/j.scitotenv.2018.07.406>.
- Arunyawat, S., Shrestha, R.P., 2016. Assessing land use change and its impact on ecosystem services in Northern Thailand. *Sustainability* 8, 22. <https://doi.org/10.3390/su8080768>.
- Arunyawat, S., Shrestha, R.P., 2018. Simulating future land use and ecosystem services in Northern Thailand. *J. Land Use Sci.* 13, 146–165. <https://doi.org/10.1080/1747423x.2018.1496157>.
- Asadolahi, Z., Salmanmahiny, A., Sakieh, Y., Mirkarimi, S.H., Baral, H., Azimi, M., 2018. Dynamic trade-off analysis of multiple ecosystem services under land use change scenarios: towards putting ecosystem services into planning in Iran. *Ecol. Complex.* 36, 250–260. <https://doi.org/10.1016/j.ecocom.2018.09.003>.
- Bao, Y.B., Liu, K., Li, T., Hu, S., 2015. Effects of land use change on habitat based on InVEST model - taking Yellow River Wetland Nature Reserve in Shaanxi province as an example. *Arid Zone Res.* 32, 622–629. <https://doi.org/10.13866/j.azr.2015.03.29>.
- Benitez-Lopez, A., Alkemade, R., Verweij, P.A., 2010. The impacts of roads and other infrastructure on mammal and bird populations: a meta-analysis. *Biol. Conserv.* 143, 1307–1316. <https://doi.org/10.1016/j.biocon.2010.02.009>.
- Cao, L., Wang, Y., Liu, C., 2021. Study of unpaved road surface erosion based on terrestrial laser scanning. *Catena (AMST)* 199. <https://doi.org/10.1016/j.catena.2020.105091>.
- Dai, F.Q., Lv, Z.Q., Zhou, Q.G., Liu, G.C., 2013. GIS-Based soil loss estimation with USLE for soil conservation planning in hilly areas of purplish soils. *Fresen. Environ. Bull.* 22, 1266–1273. <https://doi.org/10.2166/wst.2013.130>.
- Desmet, P.J.J., Govers, G., 1996. A GIS procedure for automatically calculating the USLE LS factor on topographically complex landscape units. *J. Soil Water Conserv.* 51, 427–433. [https://doi.org/10.1061/\(ASCE\)0733-9437\(1996\)122:5\(319.2\)](https://doi.org/10.1061/(ASCE)0733-9437(1996)122:5(319.2)).
- Donohue, R.J., Roderick, M.L., McVicar, T.R., 2012. Roots, storms and soil pores: Incorporating key ecohydrological processes into Budyko's hydrological model. *J. Hydrol. (AMST)* 436–437, 35–50. <https://doi.org/10.1016/j.jhydrol.2012.02.033>.
- Gong, J., Ma, X.C., Zhang, L.L., Liu, D.Q., Zhang, J.X., 2018. Spatiotemporal variation of habitat quality in Bailongjiang Watershed in Gansu based on InVEST model. *Res. Soil Water Conserv.* 25, 191–196. <https://doi.org/10.13869/j.cnki.rswc.2018.03.027>.
- González-Bernardo, E., Delgado, M.D.M., Matos, D.G.G., Zarzo-Arias, A., Morales-González, A., Ruiz-Villar, H., Skuban, M., Maiorano, L., Ciucci, P., Balbontín, J., Penteriani, V., 2023. The influence of road networks on brown bear spatial distribution and habitat suitability in a human-modified landscape. *J. Zool.* 319. <https://doi.org/10.1111/jzo.13023>.
- Guo, Z., Yan, Z., PaErHaTi, M., He, R., Yang, H., Wang, R., Ci, H., 2023. Assessment of soil erosion and its driving factors in the Huaihe region using the InVEST-SDR model. *Geocarto Int.* 38. <https://doi.org/10.1080/10106049.2023.2213208>.
- Gurung, K., Yang, J., Fang, L., 2018. Assessing ecosystem services from the forestry-based reclamation of surface mined areas in the North Fork of the Kentucky River Watershed. *Forests* 9, 23. <https://doi.org/10.3390/f9100652>.
- Hacısalihoğlu, S., Gümüş, S., Kezik, U., Karadağ, H., 2019. Impact of forest road construction on topsoil erosion and hydro-physical soil properties in a semi-arid mountainous ecosystem in Turkey. *Pol. J. Environ. Stud.* 28. <https://doi.org/10.15244/pjoes/81615>.
- Han, Y., Li, H., Liu, J., Xie, N., Jia, M., Sun, Y., Wang, S., 2023. Life cycle carbon emissions from road infrastructure in China: a region-level analysis. *Transp. Res. D Transp. Environ.* 115. <https://doi.org/10.1016/j.trd.2022.103581>.
- He, S.S., Zhu, W.B., Cui, Y.P., He, C.L., Ye, L.P., Feng, X.Y., Zhu, L.Q., 2019. Study on soil erosion characteristics of Qihe Watershed in Taihang Mountains based on the InVEST model. *Resour. Environ. Yangtze Basin* 28, 426–439.
- Hu, T.H., Chang, J., Liu, X.X., Feng, S.S., 2018. Integrated methods for determining restoration priorities of coal mining subsidence areas based on green infrastructure: a case study in the Xuzhou urban area, of China. *Ecol. Ind.* 94, 164–174. <https://doi.org/10.1016/j.ecolind.2017.11.006>.

- Kroeger, S.B., Hanslin, H.M., Lennartsson, T., D'Amico, M., Kollmann, J., Fischer, C., Albertsen, E., Speed, J.D.M., 2022. Impacts of roads on bird species richness: a meta-analysis considering road types, habitats and feeding guilds. *Sci. Total Environ.* 812 <https://doi.org/10.1016/j.scitotenv.2021.151478>.
- Kwon, Y., Choi, Y.G., Park, T., Ziegler, A., Paik, M.C., 2017. Generalized estimating equations with stabilized working correlation structure. *Comput. Stat. Data Anal.* 106, 1–11. <https://doi.org/10.1016/j.csda.2016.08.016>.
- Li, X.W., Hou, X.Y., Song, Y., Shan, K., Zhu, S.Y., Yu, X.B., Mo, X.Q., 2019a. Assessing changes of habitat quality for shorebirds in stopover sites: a case study in Yellow River Delta, China. *Wetlands* 39, 67–77. <https://doi.org/10.1007/s13157-018-1075-9>.
- Li, Y., Qi, S., Liang, B., Ma, J., Cheng, B., Ma, C., Qiu, Y., Chen, Q., 2019b. Dangerous degree forecast of soil loss on highway slopes in mountainous areas of the Yunnan-Guizhou Plateau (China) using the Revised Universal Soil Loss Equation. *Nat. Hazards Earth Syst. Sci.* 19 <https://doi.org/10.5194/nhess-19-757-2019>.
- Li, S., Wang, Z., Zhang, Y., 2017. Crop cover reconstruction and its effects on sediment retention in the Tibetan Plateau for 1900–2000. *J. Geog. Sci.* 27 <https://doi.org/10.1007/s11442-017-1406-4>.
- Li, S., Wu, J., Gong, J., Li, S., 2018. Human footprint in Tibet: assessing the spatial layout and effectiveness of nature reserves. *Sci. Total Environ.* 621, 18–29. <https://doi.org/10.1016/j.scitotenv.2017.11.216>.
- Liang, F.Y., Wang, C., Yu, X., Chinese Inst Soil, M., Geotechn Engr, S.S.C.E.A.G.I.T.R.B., Tongji, U., 2018. In: Numerical Study on the Performance of Bio-Inspired Bridge Attachments as Local Scour Countermeasures with Attack Angles. Tongji Univ, Shanghai, PEOPLES R CHINA, pp. 729–739. <https://doi.org/10.1007/978-981-13-0131-5-79>.
- Lisiak-Zielinska, M., Borowiak, K., Budka, A., 2022. How big is the real road-effect zone? The impact of the highway on the landscape structure—a case study. *Sustainability* 14. <https://doi.org/10.3390/su142215219>.
- Llagostera, P., Comas, C., Lopez, N., 2022. Modeling road traffic safety based on point patterns of wildlife-vehicle collisions. *Sci. Total Environ.* 846 <https://doi.org/10.1016/j.scitotenv.2022.157237>.
- Lv, Y., Jiang, Y., Hu, W., Cao, M., Mao, Y., 2020. A review of the effects of tunnel excavation on the hydrology, ecology, and environment in karst areas: current status, challenges, and perspectives. *J. Hydrol. (AMST)* 586. <https://doi.org/10.1016/j.jhydrol.2020.124891>.
- Matomela, N., Li, T., Ikhumhen, H.O., Lopes, N.D.R., Meng, L., 2022. Soil erosion spatio-temporal exploration and Geodetection of driving factors using InVEST-sediment delivery ratio and Geodetector models in Dongsheng, China. *Geocarto. Int.* 37, 13039–13056. <https://doi.org/10.1080/10106049.2022.2076912>.
- Mayer, M., Fischer, C., Blaum, N., Sundt, P., Ullmann, W., 2022. Influence of roads on space use by European hares in different landscapes. *Landsc. Ecol.* <https://doi.org/10.1007/s10980-022-01552-3>.
- Mulero-Pazmany, M., Rollan, L., D'Amico, M., Gonzalez-Suarez, M., 2023. Road orientation affects the impact of roads on wildlife. *Wildl. Res.* 50, 39–46. <https://doi.org/10.1071/wr21149>.
- Oliveira Gonçalves, L., Kindel, A., Bastazini, V.A.G., Zimmermann Teixeira, F., 2022. Mainstreaming ecological connectivity in road environmental impact assessments: a long way to go. *Impact Assess. Project Apprais.* <https://doi.org/10.1080/14615517.2022.2099727>.
- Onder, H., 2016. Comparative study of generalized estimating equations and logistic regressions on different sample sizes and correlation levels. *Commun. Stat.-Simul. Comput.* 45, 3528–3533. <https://doi.org/10.1080/03610918.2015.1010000>.
- Pan, T., Wu, S.H., Dai, E.F., Liu, Y.J., 2013. Spatiotemporal variation of water source supply service in Three River Source area of China based on InVEST model. *Chin. J. Appl. Ecol.* 24, 183–189. <https://doi.org/10.13287/j.1001-9332.2013.0140>.
- Phillips, B.B., Bullock, J.M., Osborne, J.L., Gaston, K.J., 2020. Ecosystem service provision by road verges. *J. Appl. Ecol.* 57, 488–501. <https://doi.org/10.1111/1365-2664.13556>.
- Ran, C., Wang, S., Bai, X., Tan, Q., Zhao, C., Luo, X., Chen, H., Xi, H., 2020. Trade-offs and synergies of ecosystem services in Southwestern China. *Environ. Eng. Sci.* 37, 669–678. <https://doi.org/10.1089/ees.2019.0499>.
- Rao, Y., Zhang, J., Xu, Q., Wang, S., 2018. Sustainability assessment of road networks: a new perspective based on service ability and landscape connectivity. *Sustain. Cities Soc.* 40, 471–483. <https://doi.org/10.1016/j.scs.2018.05.013>.
- Shaffer, J.A., Roth, C.L., Mushet, D.M., 2019. Modeling effects of crop production, energy development and conservation-grassland loss on avian habitat. *PLoS One* 14. <https://doi.org/10.1371/journal.pone.0198382>.
- Sharp, R., Tallis, H.T., Ricketts, T., Guerry, A.D., Wood, S.A., Chaplin-Kramer, R., Nelson, E., Ennaanay, D., Wolny, S., Olwero, N., Vigerstol, K., Pennington, D., Mendoza, G., Aukema, J., Foster, J., Forrest, J., Cameron, D., Arkema, K., Lonsdorf, E., Kennedy, C., Verutes, G., Kim, C.K., Guannel, G., Papenfus, M., Toft, J., Marsik, M., Bernhardt, J., Griffin, R., Glowinski, K., Chaumont, N., Perelman, A., Lacayo, M., Mandl, L., Hamel, P., Vogl, A.L., Rogers, L., Bierbower, W., Denu, D., Douglass, J., 2018. InVEST 3.5.0 User's Guide.
- Terrado, M., Sabater, S., Chaplin-Kramer, B., Mandl, L., Ziv, G., Acuna, V., 2016. Model development for the assessment of terrestrial and aquatic habitat quality in conservation planning. *Sci. Total Environ.* 540, 63–70. <https://doi.org/10.1016/j.scitotenv.2015.03.064>.
- Trisurat, Y., Eawpanich, P., Kalliola, R., 2016. Integrating land use and climate change scenarios and models into assessment of forested watershed services in Southern Thailand. *Environ. Res.* 147, 611–620. <https://doi.org/10.1016/j.envres.2016.02.019>.
- Uliasz-Misiak, B., Winid, B., Lewandowska-Smierczalska, J., Matula, R., 2022. Impact of road transport on groundwater quality. *Sci. Total Environ.* 824 <https://doi.org/10.1016/j.scitotenv.2022.153804>.
- van der Ree, R., Jaeger, J.A.G., van der Grift, E.A., Clevenger, A.P., 2011. Effects of roads and traffic on wildlife populations and landscape function: road ecology is moving toward larger scales. *Ecol. Soc.* 16.
- Wang, Y., Guan, L., Chen, J.D., Kong, Y.P., 2018. Influences on mammals frequency of use of small bridges and culverts along the Qinghai-Tibet railway, China. *Ecol. Res.* 33, 879–887. <https://doi.org/10.1007/s11284-018-1578-0>.
- Wang, Y., He, W., Zhang, T., Zhang, Y.N., Cao, L.X., 2022. Adapting the WEPP hillslope model and the TLS technology to predict unpaved road soil erosion. *Int. J. Environ. Res. Public Health* 19. <https://doi.org/10.3390/ijerph19159213>.
- Wang, Z.M., Li, Q.Z., Liu, L., Zhao, H.L., Ru, H.E., Wu, J.P., Deng, Y.L., 2023. Spatiotemporal evolution and attribution analysis of water yield in the xiangjiang river basin (XRB) based on the InVEST model. *Water (Basel)* 15. <https://doi.org/10.3390/w15030514>.
- Wang, S.J., Yan, X.M., Zhang, C., Meng, L., Yang, K., 2016. Hierarchical object method of highway route selection in permafrost region. *J. Traffic Transport. Eng.* 16, 1–13. <https://doi.org/10.19818/j.cnki.1671-1637.2016.04.001>.
- Wei, P.J., Chen, S.Y., Wu, M.H., Deng, Y.F., Xu, H.J., Jia, Y.L., Liu, F., 2021. Using the InVEST model to assess the impacts of climate and land use changes on water yield in the upstream regions of the shule river basin. *Water (basel)* 13, 20. <https://doi.org/10.3390/w13091250>.
- Wei, J.Q., Zhang, Y., Liu, Y., Li, C., Tian, Y.S., Qian, J., Gao, Y., Hong, Y.S., Liu, Y.F., 2022. The impact of different road grades on ecological networks in a mega-city Wuhan City, China. *Ecol. Indic.* 137 <https://doi.org/10.1016/j.ecolind.2022.108784>.
- Wu, C.F., Lin, Y.P., Chiang, L.C., Huang, T., 2014. Assessing highway's impacts on landscape patterns and ecosystem services: a case study in Puli Township, Taiwan. *Landsc. Urban Plan* 128, 60–71. <https://doi.org/10.1016/j.landurbplan.2014.04.020>.
- Wu, J.H., Liu, S.Y., Bai, S., 2021. Identification and optimization of ecological corridors in Shenmu City based on landscape ecological security. *Arid. Zone Res.* 1–9. <https://doi.org/10.13866/j.azr.2021.04.24>.
- Yan, Z., You, N., Wang, L., Lan, C., 2023. Assessing the impact of road network on urban landscape ecological risk based on corridor cutting degree model in Fuzhou, China. *Sustainability* 15. <https://doi.org/10.3390/su15021724>.
- Yang, X., Chen, R.S., Meadows, M.E., Ji, G.X., Xu, J.H., 2020. Modelling water yield with the InVEST model in a data scarce region of northwest China. *Water Supply* 20, 1035–1045. <https://doi.org/10.2166/ws.2020.026>.
- Yu, Y.H., Sun, X.Q., Wang, J.L., Zhang, J.P., 2022. Using InVEST to evaluate water yield services in Shangri-La, Northwestern Yunnan, China. *PeerJ*, 20, 21. <https://doi.org/10.7717/peerj.12804>.
- Yue, W.Z., Xiong, J.H., Liu, Y., Xia, H.X., 2022. Ecosystem services dynamics towards SDGs in the belt and road Initiative cities. *Prog. Phys. Geogr.-Earth Environ.* <https://doi.org/10.1177/03091333221118364>.
- Zhang, Z.L., Liu, S.L., Zhao, Q.H., Yang, Y.J., 2010. Effects of road network on landscape ecological risk: a case study of Red River Watershed. *Chin. J. Ecology* 29, 2223–2228. <https://doi.org/10.13292/j.1000-4890.2010.0331>.

- Zhang, C., Yang, K., Wang, S.J., Yang, H.Z., Shao, G.J., 2016. Highway intelligent route selection method in permafrost region of Qinghai-Tibet Plateau. *J. Traffic Transport. Eng.* 16, 14–25. <https://doi.org/10.19818/j.cnki.1671-1637.2016.04.002>.
- Zhang, H., Zhang, C., Hu, T., Zhang, M., Ren, X., Hou, L., 2020. Exploration of roadway factors and habitat quality using INVEST. *Transp. Res. D Transp. Environ.* 87, 102551 <https://doi.org/10.1016/j.trd.2020.102551>.
- Zhao, S., Yan, Y., Han, J., 2021. Industrial land change in chinese silk road cities and its influence on environments. *Land (Basel)* 10. <https://doi.org/10.3390/land10080806>.
- Zheng, X., Zou, Z., Xu, C., Lin, S., Wu, Z., Qiu, R., Hu, X., Li, J., 2022. A New remote sensing index for assessing spatial heterogeneity in urban ecoenvironmental-quality-associated road networks. *Land (Basel)* 11. <https://doi.org/10.3390/land11010046>.
- ZhuGe, H.M., Li, X.W., Zhang, Z., Gao, F., Xu, D.H., 2014. Identification and conservation assessment of suitable habitats for Tibet antelope in the alpine desert, Qinghai-Tibet Plateau. *Chin. J. Appl. Ecol.* 25, 3483–3490. <https://doi.org/10.13287/j.1001-9332.20141009.003>.